Self-radiation effects and glassy nature of magnetic transition in AmO_2 revealed by ^{17}O-NMR

Yo Tokunaga,[1,*] Tsuyoshi Nishi,[2] Masami Nakada,[2] Akinori Itoh,[2] Hironori Sakai,[1] Shinsaku Kambe,[1] Yoshiya Homma,[3] Fuminori Honda,[3] Dai Aoki,[3] and Russell E. Walstedt[4]

[1]*Advanced Science Research Center, Japan Atomic Energy Agency, Tokai, Ibaraki 319-1195, Japan*
[2]*Nuclear Science and Engineering Directorate, Japan Atomic Energy Agency, Tokai, Ibaraki 319-1195, Japan*
[3]*Institute for Materials Research, Tohoku University, Oarai, Higashi-Ibaraki, Ibaraki 311-1313, Japan*
[4]*Physics Department, The University of Michigan, Ann Arbor, Michigan 48109, USA*

(Received 18 April 2014; revised manuscript received 27 May 2014; published 19 June 2014)

The magnetic phase transition near $T_0 = 8.5$ K in americium dioxide (AmO_2) has been investigated microscopically by means of ^{17}O NMR. To avoid complexities arising from sample aging associated with the α decay of ^{243}Am, all measurements have been performed within 40 days after sample synthesis. Even during such a short period, however, a rapid change of NMR line shape has been observed at 1.5 K, suggesting that the ground state of AmO_2 is very sensitive to disorder. We have also confirmed the loss of ^{17}O NMR signal intensity over a wide temperature range below T_0, and more than half of oxygen nuclei are undetectable at 1.5 K. This behavior reveals the persistence of slow and distributed spin fluctuations down to temperatures well below T_0. In the paramagnetic state, strong NMR line broadening and spatially inhomogeneous spin fluctuations have been observed. The results are all indicative of short-range, spin-glass-like character for the magnetic transition in this system.

DOI: 10.1103/PhysRevB.89.214416 PACS number(s): 75.50.Lk, 76.60.−k, 71.27.+a, 74.62.En

I. INTRODUCTION

Intensive studies have been made to elucidate the electronic properties of Actinide dioxides (AnO_2, An = actinide). Their importance stems not only from technological considerations, but also from a fundamental interest in understanding the basic properties of strongly correlated $5f$ electrons in solids. Among the AnO_2, low-temperature phase transitions have been discovered in UO_2, NpO_2, and AmO_2. UO_2 exhibits long-range, triple-q antiferromagnetic (AFM) order below $T_N = 30$ K [1–5]. This AFM order has been found to be accompanied by antiferroquadrupolar order, as well as internal distortion of the oxygen cube [5–8]. On the other hand, NpO_2 exhibits rather exotic order, that is, a spontaneous ordering of octupoles (or, possibly, higher-order Γ_5 multipoles) below $T_0 = 26$ K [9–16]. In the ordered state, neither long-range magnetic dipole order [17,18] nor structural distortion [19] appears. Resonant x-ray scattering [12] and nuclear magnetic resonance (NMR) [15,16] both played a critical role in understanding this new class of ordered multipolar ground states.

In AmO_2, the magnetic phase transition near $T_0 = 8.5$ K is far less clearly understood compared with the other two AnO_2 systems. This transition was discovered via magnetic susceptibility measurements more than 30 years ago [20]. It was originally suggested to be AFM order in analogy with the phase transition in UO_2. However, such a simple picture of AFM order was doubted after two microscopic measurements appeared, i.e., ^{243}Am Mössbauer spectroscopy [21] and neutron scattering [22]. Both measurements failed to detect statically ordered Am dipole moments below T_0. On the other hand, the crystalline electric field (CEF) ground state of Am^{4+} ($5f^5$) had been suggested to be a Γ_7 doublet for AmO_2 [20,23–25]. The Γ_7 doublet state carries only a dipolar degree of freedom, and thus nondipolar ordering was not expected. Recently, however, it has been pointed out theoretically that the CEF ground state can easily be converted into a Γ_8 quartet through a competition between spin-orbit coupling and Coulomb interactions [26,27]. Since the Γ_8 quartet carries not only dipole but also quadrupole and octupole moments, the possibility of multipolar ordering has also been proposed [26–28].

However, there is another serious limitation on studies of Am compounds that must be addressed, and which turns out to dominate the outcome of experimental studies such as we report in this paper. This is the strong self-radiation crystalline disorder effect caused by α-particle decay of Am. The ^{243}Am nuclide has a half-life of $t_{1/2} = 7370$ years; it decays into an α particle and a recoiling ^{239}Np ion [29–31]. The light α particle creates displacements over a long range, while the heavy recoiling daughter ion causes severe damage in a local region, although some of this recovers in a short time via lattice vibrations. It has been estimated that each event creates 1000–1500 Frenkel-pair defects consisting of a lattice vacancy and an interstitial atom. The accumulation of self-radiation damage at room temperature results in lattice expansion over time [32], which saturates after about 600 days for the case of $^{243}AmO_2$.

In a previous paper, we have reported the results of ^{17}O NMR performed using an aged sample of $^{243}AmO_2$ [33]. Those NMR data provided microscopic evidence for a magnetic phase transition around $T_0 \sim 8.5$ K as a bulk property of this system. However, since our sample had already been stored about 600 days prior to the NMR measurements, it was necessary to assume that the crystalline state of the aged sample had been substantially modified from its original form. Indeed, our NMR data revealed the existence of widely distributed hyperfine fields at oxygen sites. Thus, in the present work, we have performed ^{17}O NMR on a newly synthesized $^{243}AmO_2$ powder sample. All NMR measurements have been performed within 40 days after sample synthesis in an effort

*tokunaga.yo@jaea.go.jp

to avoid complexities that accrue from sample aging. Even in such a short period of time, we have observed a rapid change of the ^{17}O NMR spectrum at 1.5 K, demonstrating that the electronic ground state of this system is highly sensitive to disorder. We have also confirmed substantial loss of NMR signal intensity over a wide temperature range around T_0. This phenomenon, known as "signal wipeout," indicates the presence of slow spin fluctuations occurring inhomogeneously throughout the sample. All our results display the signature of a short-range, spin-glass-like character for magnetic ordering in our sample of AmO_2.

II. EXPERIMENTAL RESULTS

A. Sample preparation

An ^{17}O-enriched $^{243}AmO_2$ powder sample has been prepared by heating ^{243}AmN powder at 973 K in an atmosphere of O_2 gas containing 90 at. % ^{17}O. X-ray-diffraction patterns confirmed the cubic fluorite AmO_2 structure for our sample material. The NMR sample – about 5.6 mg of AmO_2 powder, amounting to 37 MBq – was wrapped with polyimide tape and encapsulated in a polyimide tube using epoxy resin. The encapsulated sample in the tube was then doubly sealed in a Teflon capsule, again using epoxy resin. The series of sealing procedures along with sample transportation required 13 days prior to starting NMR measurements; the sample has been at room temperature during that period. All the NMR measurements reported here have been performed within one month after the sample was installed in a cryostat.

B. Aging effects

^{17}O NMR measurements have been performed using a phase coherent, pulsed spectrometer. The ^{17}O nucleus has $I = 5/2$ with a gyromagnetic ratio $\gamma_N = 5.7719$ MHz/T. Field-swept NMR spectra were taken at a frequency of $f_{NMR} = 30.3$ MHz with external fields of ∼5 T. Spin-lattice relaxation times T_1 were measured using the saturation-recovery method.

Aging effects have been examined by comparing ^{17}O NMR spectra measured at temperatures of 1.5, 9, and 210 K in the first and last stages of the investigation. Figure 1 shows the spectra at 1.5 K on (a) the first day (about 10 h after installing the sample in a cold dewar) and (b) after 26 days. During the period between (a) and (b), the sample was in a cryostat where the sample temperature was maintained mostly below 50 K. As seen in Fig. 1(a), we have observed a hybrid spectrum consisting of a narrow (N) and a broad (B) component on the first day. The full width at half maximum (FWHM) of these components is about 0.1 and 7 kOe, respectively, and the ratio of the integrated intensity of the two components is $I_N : I_B \simeq 1 : 9$. After 26 days, on the other hand, we have observed only the broad component of the spectrum, as shown in Fig. 1(b). The triangular line shape with a base of ∼14 kOe, is very similar to the one observed in our previous study on the 600-day-old aged sample [33], indicating that the internal local fields H_{int} at oxygen sites are distributed very nearly randomly from zero to a maximum value $H_{int}^{max} \sim 7$ kOe.

On the other hand, as shown in Fig. 2(a), no appreciable change was observed with sample aging in the paramagnetic

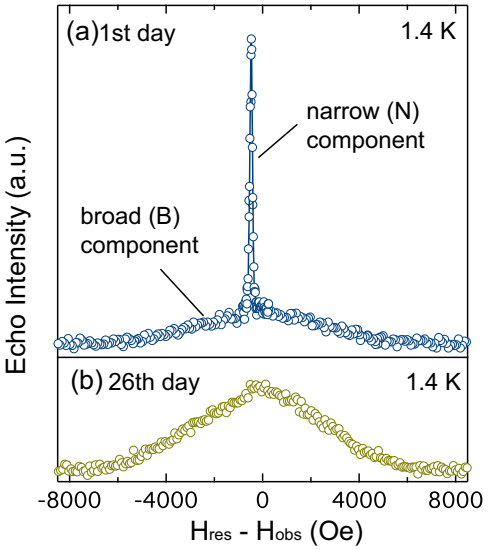

FIG. 1. (Color online) ^{17}O NMR spectra obtained at 1.5 K on (a) the first day (about 10 h after installing the sample in a cold dewar) and (b) 26 days later. The horizontal axis $H_{res} - H_{obs}$ corresponds to the magnitude of the internal field at ^{17}O nuclei H_{int}, where $H_{res} = f_{NMR}/\gamma_N$ and H_{obs} is the observing field.

state at 9 K. This was also the case at 210 K. A single, symmetric NMR peak has been observed at all temperatures above 8.5 K. The linewidth was found to be about half of

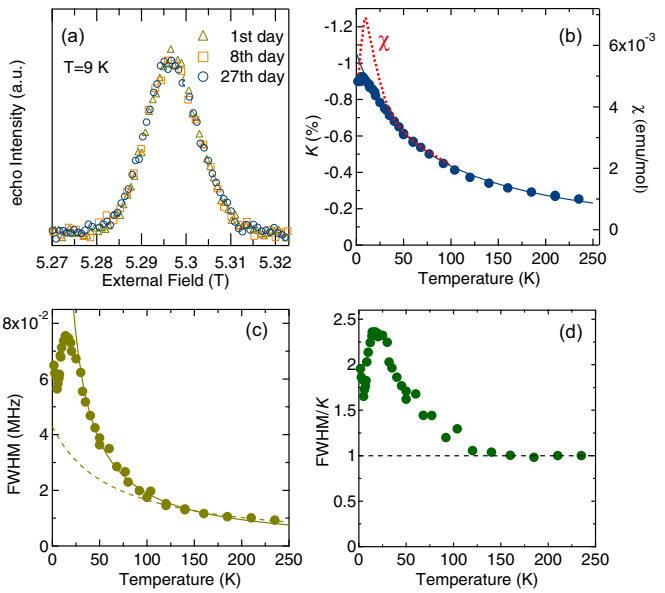

FIG. 2. (Color online) (a) Comparison of field-sweep ^{17}O NMR spectra measured on the 1st, 8th, and 27th days of the experiment at 9 K. (b) Temperature dependence of the Knight shift K. The solid line indicates a Curie-Weiss (CW) fit to the data with $\theta = -70$ K, and the dotted line shows the temperature dependence of the bulk susceptibility [20]. (c) Temperature dependence of the FWHM. The solid line indicates a CW fit to the data in the 20–100 K temperature range with $\theta \sim 0$ K, while the dotted line shows a CW fit to the data above 100 K with $\theta \sim -70$ K. (d) The temperature dependence of the ratio of the FWHM to the Knight shift, FWHM/K. The ratio is normalized to unity at ∼250 K.

that obtained in the previous, 600-day-old sample, suggesting that the spectrum in the paramagnetic state can also be broadened by self-radiation damage over longer periods of years.

The results in Fig. 1 illustrate some important points about the nature of the magnetic state of our sample of AmO_2 and how it evolves with the passage of time. The narrow line in Fig. 1(a) is from the portion of the sample that is effectively in a paramagnetic state, i.e., there is no sign of magnetic order. At higher temperatures other NMR spectra are shown and discussed, and we note with emphasis that all such spectra will be from the paramagnetic region of the sample with linewidths of the order of 50–100 Oe at temperatures in the vicinity of T_0 or lower. There are two other identifiable regions of the sample, and these are also evident in Fig. 1. First, there is the region that has entered into a spin-glass ordered state, corresponding to the broad background lines. Such regions exhibit line broadening that is ∼two orders of magnitude greater than the paramagnetic region. As will be discussed in greater detail below, this large broadening effect is a consequence of fixed Am^{4+} magnetic moments that characterize spin-glass magnetic order. Because of their random orientation, the cancellation of dipolar hyperfine (HF) fields that takes place with essentially uniform induced moments in the paramagnetic region is no longer effective. This unleashes the enormous broadening power of dipolar fields from the enhanced $5f$-$2p$ hybridization that occurs in this system. A third region of the sample is characterized by slow magnetic fluctuations of such a nature that nearby ^{17}O nuclear spins are relaxed too quickly for their NMR signal to be observable. This effect is often referred to as "wipeout" and is a major influence in our NMR spectroscopy of AmO_2. We discuss this effect in detail below, but for the present we note that wipeout is responsible for the lower amplitude ordered-state NMR line in Fig. 1(a) as compared with Fig. 1(b). As the sample ages, a larger fraction of sample volume is converted into statically ordered spin glass at 1.5 K, so that the broad line has greater intensity after 26 days than at the beginning of the study.

C. Signal wipeout

Figure 3 shows the temperature variation of the NMR spectra between (a) 30 and 12 K and (b) 12 and 4.2 K, respectively. In order to compare their relative intensities over a range of temperatures, the signal intensity of each spectrum is normalized to a constant Boltzmann factor $1/T$ for nuclear polarization. With decreasing temperature, the height of the spectrum is suppressed but the width is increased between 30 and 12 K. On the other hand, amplitude suppression occurs without spectral broadening below 12 K. Thus, we lose significantly more NMR signal intensity below 12 K. Some of the intensity loss is to wipeout and some is to the broad spin-glass NMR line.

In Fig. 3(c), we plot the temperature dependence of the integrated spectral intensity (I) multiplied by temperature (T). Intensities I are obtained by integrating each region of the full spectrum after making T_2 corrections to signal amplitudes. T_2 corrections are required for all pulsed NMR experiments, since the observation occurs at a finite time after the rephasing

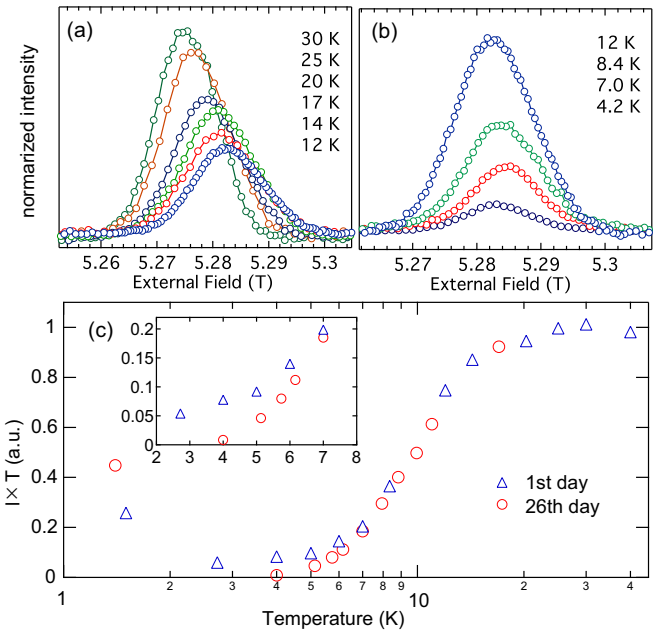

FIG. 3. (Color online) Comparison of the NMR spectra obtained at several different temperatures between (a) 30 and 12 K and (b) 12 and 4.2 K, respectively. In order to compare the relative intensity among different temperatures, the signal intensity is normalized to a constant Boltzmann factor $1/T$. (c) Temperature dependence of the integrated spectrum intensity (I) multiplied by T. The data were taken on the 1st and 26th days in our experiment. The inset shows the behavior between 2 and 8 K in more detail.

rf pulse. Thus, the measured signal should be extrapolated back to its maximum initial value.

After T_2 corrections, the product IT is proportional to the number of nuclei observed, and hence should be temperature independent. However, loss of the normalized intensity IT has often been observed in NMR experiments. A major mechanism for such losses is a dramatic shortening of T_2. Thus, T_2 for some fraction of the nuclei becomes shorter than the dead time of the spectrometer (typically ∼a few microseconds), so that one cannot correct for this by extrapolating the signal intensity back to zero. For nuclei whose signal is lost in this way, the signal is said to be "wiped out."

As seen in Fig. 3(c), the loss of IT starts gradually below 20 K, then increases drastically below $T \sim 12$ K. Signal intensity partially recovers as the broad spin-glass NMR line at the lowest temperature of 1.5 K, but there more than half of the oxygen nuclei are not detected. Interestingly, we have also observed a small but distinct aging effect for IT below 6 K, as seen in the inset of Fig. 3(c). For the first cooling, the sharp NMR line, accompanied with a very tiny broad component, has finite intensities over the whole temperature region, although its amplitude was drastically reduced at temperatures below 8.5 K. At ∼1.5 K, IT recovers slightly up to ∼25%, due entirely to the broad component. For the second cooling after one month, however, the sharp NMR signal disappeared completely around 4 K. On the other hand, at 1.5 K the broad component recovers more rapidly and IT reaches ∼45% of its high-temperature value.

D. Knight shift and FWHM

In Fig. 2(b), we plot the temperature dependence of the Knight shift determined from the position of the spectral peak. In the AnO_2 series, owing to the local tetrahedral symmetry at O sites, direct dipolar HF fields from the four nearest-neighbor Am^{4+} moments all cancel out in the paramagnetic state. The $5f$-$2p$ hybridization transfer between Am and O orbitals therefore has no effect on the shift and may affect the linewidth only through crystalline disorder. The ample Knight-shift effect must therefore originate through a small hybridization spin transfer $5f$-$3s$. Although this is undoubtedly much smaller than the spin transfer to the oxygen $2p$ orbitals, its effect is substantial, because the s-contact HF field is quite large and because contributions from the four nearest-neighbor Am^{4+} ions add linearly with no cancellation. A very small and weakly T-dependent Knight shift has been observed in both UO_2 and NpO_2 [5,15]. Those results indicate that the orbital hybridization is relatively much smaller in these early members of the series. The present results are consistent with a recent theoretical calculation that has predicted a rapid increase of orbital hybridization associated with $5f$–O $2p$ orbital energy degeneracy in the middle members of the dioxide series, PuO_2, AmO_2, and CmO_2 [34]. We suggest that the s-contact hybridization would be proportionately larger as well. The negative Knight-shift value reveals the negatively polarized character of the s-contact spin transfer to O orbitals, originating from the Hund's rules ground state of $^6H_{5/2}$ for Am $5f$ electrons ($J = L - S$).

The solid line in Fig. 2(b) shows a fit to a Curie-Weiss (CW) law, $K = C/(T - \theta)$ with $\theta = -70$ K. The CW behavior is consistent with a localized picture for the Am $5f$ moments, where the negative θ value indicates that exchange coupling between the $5f$ moments is AFM in character. In the same figure we also plot the temperature dependence of the bulk susceptibility (dotted line) reported in Ref. [20]. The Knight-shift behavior is scaled to the bulk susceptibility $\chi(T)$ above 40 K, but shows a clear deviation below that temperature. From the scaling behavior, we can estimate the hyperfine coupling constant to be $A = -9.4$ kOe/μ_B. This value is much larger than those obtained in UO_2 and NpO_2, confirming a larger s-contact transferred HF field. The failure of $K(T)$ to follow $\chi(T)$ below $T \sim 40$ K is attributed to the loss of ^{17}O NMR signal in regions of the sample that yield the highest magnetic polarization at these temperatures (see discussion of wipeout effects above).

Figure 2(c) shows the temperature dependence of the full width at half maximum (FWHM) in the paramagnetic region. Above 200 K, the FWHM is only about 10 kHz, which is comparable with that obtained for UO_2 and NpO_2 at similar fields and temperatures [35], and hence, confirms the high quality of the present AmO_2 sample. With decreasing temperature, the FWHM increases rapidly below 100 K and shows a maximum around 14 K. The FWHM above 100 K can be fitted to the CW law with $\theta \sim -70$ K; the same value as for the Knight shift. On the other hand, the CW fit to the data in the 20–100-K temperature range gives a value $\theta \sim 0$ K. Interestingly, the FWHM shows a better scaling with the bulk susceptibility over a wide temperature region than the shift. In Fig. 2(d), we plot the ratio of the FWHM to the Knight shift against temperature. The ratio is nearly constant at higher temperatures, but strongly enhanced at temperatures below 100 K. The faster increase of the linewidth compared with the Knight shift suggests the development of spatial inhomogeneity in the static susceptibility at low temperatures. Over a similar temperature range, we have also observed the development of dynamical inhomogeneity, as discussed in the next section.

E. Dynamical inhomogeneity

The development of the dynamical inhomogeneity has been confirmed by measuring the nuclear spin-lattice and spin-spin relaxation rates, $1/T_1$ and $1/T_2$ at several different positions on a broadened spectrum, as shown in Fig. 4. In these measurements, we chose a relatively long excitation pulse of 100 μsec in order to excite a relatively narrow spectral bandwidth of about 10 Oe, which is a small fraction of the full width ~100 Oe of the spectrum. The relaxation of nuclear magnetization within such narrow ranges was found to exhibit an exponential decay for T_1 and T_2. The lack of appreciable spectral diffusion indicates that the line broadening is local in character, i.e., neighboring ^{17}O spins are detuned from one another. As seen in Fig. 4, both $1/T_1$ and $1/T_2$ successively increase with increasing $|K|$, and become the largest at the edge of the spectrum where $|K|$ has the largest value. This confirms the existence of spatially inhomogeneous HF field fluctuations, linked with the NMR line broadening near T_0.

It might be not very surprising that the distribution of static hyperfine fields causes a distribution of HF field fluctuations. However, we emphasize that further development of the dynamical inhomogeneity with different strengths of magnetic correlations exists in this system. This has been suggested by highly contrasting $1/T_1$ behaviors observed at different points in the spectrum, as shown in Fig. 5. Above 8.5 K, we measured $1/T_1$ at two different positions corresponding to $K_L = 0.9 \times K$ and $K_H = 1.2 \times K$ (see Fig. 4; K is the Knight-shift value determined from the peak position for each spectrum). Below 40 K the behavior of $1/T_1$ is very different at K_L and K_H. We have observed flat $1/T_1$ behavior at K_L ($1/T_{1,L}$), as expected from a relaxation process generated by

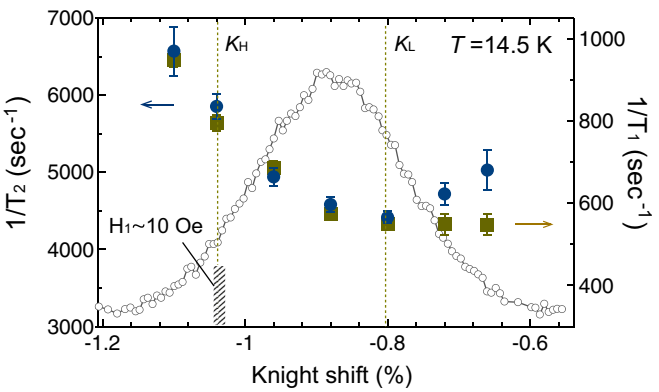

FIG. 4. (Color online) The K dependence of the nuclear spin-lattice relaxation rate $1/T_1$ and of the spin-spin rate $1/T_2$ at 14.5 K. The dotted lines at $K_L = 0.9 \times K$ and $K_H = 1.2 \times K$ correspond to the positions on the spectrum profile (circles) where the temperature dependence was measured (see text and Fig. 5).

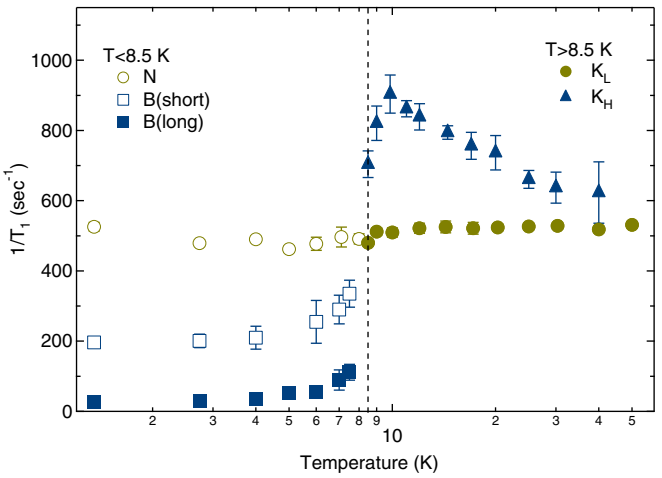

FIG. 5. (Color online) Temperature dependence of $1/T_1$. Above 8.5 K, $1/T_1$ has been measured at two different shift values corresponding to $K_L = 0.9 \times K$ and $K_H = 1.2 \times K$. Below 8.5 K, we measured $1/T_1$ for the narrow (N) and broad (B) portions of the spectrum (see Fig. 1). For the broad spectrum, which exhibits a spectrum of decay rates, we plot the shortest and longest T_1 components present.

the fluctuations of exchange-coupled local moments. On the other hand, $1/T_1$ behavior at K_H $(1/T_{1,H})$ shows an upturn with decreasing temperature and shows a maximum around 10 K, just above T_0. This behavior is attributed to slowing down of the fluctuating moments and thus is associated with a magnetic transition. However, the upturn is rather broad and small compared to that observed for the uniform AFM transition in UO_2, although both compounds show a sharp drop in $1/T_1$ below the transition. Critical slowing down of magnetic fluctuations in UO_2 causes a very sharp and strong peak in $1/T_1$ just above T_N [5]. $1/T_{1,L}$ and $1/T_{1,H}$ merge into the same value at higher temperatures, indicating that dynamical inhomogeneity only develops below ~40 K. The magnetic transition at $T \simeq 8.5$ K is suggested to be of a spin-glass nature.

In the ordered state below $T_0 = 8.5$ K, we have measured $1/T_1$ for the narrow and broad components of the spectrum (see Fig. 1). $1/T_1$ for the narrow component, $(1/T_1)_n$, is temperature independent and connects smoothly to the flat T_1 behavior at K_L. This strongly suggests that the narrow component of the spectrum arises from nuclei remaining in the paramagnetic state (no magnetic gap). On the other hand, the recovery of the nuclear magnetization of the broad component $(1/T_1)_b$ shows nonexponential behavior; in this case we have extracted the shortest and longest T_1 components from the recovery at each temperature. As seen in Fig. 5, the long component is suppressed rapidly with decreasing temperature below T_0, suggesting the opening of a magnetic excitation gap in this region. In contrast, the short component converges to a constant value at low T, suggesting that in that region magnetic fluctuations persist to well below the magnetic ordering temperature.

From the $1/T_1$ behavior in Fig. 5, it is suggested that there are two different regions in our sample, that is, one in the paramagnetic state $[1/T_{1,L}$ and $(1/T_1)_n]$ and another with random-orientation spin freezing or randomly oriented AFM clusters (a cluster spin glass) [36,37] $[1/T_{1,H}$ and $(1/T_1)_b]$. However, the interpretation is more complex than this, since the wipeout region dominates a major fraction of the sample volume below 6 K, as discussed in the foregoing section. Therefore, we should consider that $(1/T_1)_n$ and $(1/T_1)_b$ obtained here only represent the spin dynamics in two particular regions where magnetic correlation develops most rapidly and slowly, respectively, in our sample. We will discuss this point in detail below.

III. DISCUSSION

The NMR signal wipeout observed here is attributed to a dynamical effect, a dramatic shortening of T_2. In general, T_2 reflects the irreversible dephasing of the nuclear spins during spin-echo formation. This dephasing can be caused by the dipolar interaction between nuclear spins and/or dynamic hyperfine coupling with electronic spins. T_2 decay by the former process is temperature independent in a stable environment. Under a magnetic transition, the dynamic spin-spin relaxation cannot be inhibited by magnetic detuning of neighboring spins. Dynamic T_2 relaxation via HF coupling with atomic magnetic moments is a likely mechanism in a disordered magnetic system such as a spin glass.

In terms of the spectral density of the fluctuating hyperfine field at zero frequency, $1/T_2$ via the latter process may be expressed as [38]

$$1/T_2 = \gamma_N^2 \langle h_z^2 \rangle \tau(T), \tag{1}$$

where γ_N is the nuclear gyromagnetic ratio of the observed nuclei, h_z is the local longitudinal fluctuating hyperfine field at the site of the nucleus, and τ is the correlation time of the electron moment fluctuations. Equation (1) is valid in the fast motion limit, i.e., $\gamma_N(\langle h_z^2 \rangle)^{1/2}\tau \ll 1$. On approaching a magnetic transition, $\tau(T)$ increases rapidly and hence T_2 can shorten dramatically. NMR signal wipeout then occurs when τ reaches a critical value τ_1 where the time scale of T_2 becomes shorter than the dead time of the spectrometer, i.e., less than several microseconds (e.g., τ_1 is about 10^{-8} sec with a typical value of $\langle h_z^2 \rangle \sim 10^{-1}$ T). With further decrease of temperature, $\tau(T)$ enters the slow motion regime, $\gamma_N(\langle h_z^2 \rangle)^{1/2} \lesssim 1/\tau$. In this regime, T_2 increases with increasing $\tau(T)$, and the NMR signal can again become observable if $\tau(T)$ exceeds another critical value τ_2, where $\tau_2 \sim T_2 \sim 10^{-6}$ sec. Between τ_1 and τ_2, the NMR spin echo is undetectable due to its extremely short T_2 value.

In a crystalline magnet, long-range magnetic correlation develops homogeneously over the entire sample volume. $\tau(T)$ for all the nuclei then passes through the critical region of the wipeout rapidly, so that the loss of NMR signal occurs only in a very narrow temperature region. On the other hand, if only short-range magnetic correlations appear in the sample, then the fluctuation spectrum will be distributed over a wide frequency range. In addition, owing to the short-range character of the correlations, slow spin fluctuations will generally persist down to very low temperatures. As a result, signal wipeout will then occur over a relatively wide temperature range. Strong wipeout effects have been observed

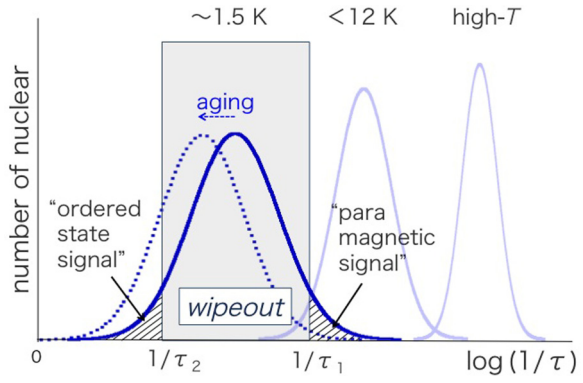

FIG. 6. (Color online) A hypothetical temperature dependence for the fluctuation spectrum in AmO_2.

in classical spin-glass systems [39–41] and the stripe-ordered cuprates [42–45], etc.

Signal wipeout indeed appears over a wide temperature range in AmO_2, demonstrating the short-range, inhomogeneous character of the magnetic transition. Figure 6 illustrates a hypothetical temperature variation of the fluctuation spectrum expected from the IT and T_1 behaviors. Here we have assumed a simple Lorentzian distribution for the fluctuation spectrum. At temperatures decreasing below 40 K, the fluctuation spectrum gradually broadens and shifts to lower frequency. Around 20 K, the tail of the fluctuation spectrum reaches the critical region for wipeout and the loss of the NMR signal begins among the most vulnerable nuclei and spreads throughout the sample. The spectrum is also broadening with decreasing temperature, leading to drastic NMR signal loss in the wipeout region below T_0. Finally, at 1.5 K the fluctuation spectrum becomes so wide that its tails cover both the "paramagnetic ($\tau < \tau_1$)" and "ordered state ($\tau > \tau_2$)" regions. As a result, we observe a hybrid spectrum consisting of the narrow and the broad components, even though most of nuclei are still in the wipeout region.

Pursuing this picture, we can also understand the aging effect on the NMR spectrum at 1.5 K rather simply as being caused by a small shift of the fluctuation spectrum to lower frequency. As shown in Fig. 6, such a shift decreases the paramagnetic signal, while increasing the ordered state signal, although many of the nuclei are still in the wipeout region. This result implies that the self-radiation damage effect tends not to weaken, but to stabilize the magnetic ordering in this system.

So the magnetic order in our AmO_2 sample is characterized as a kind of "disorder-induced" spin-glass magnetism. To understand this disordering process, we need detailed knowledge of the self-radiation damage expected to accumulate as our sample ages. As noted above, each event of the α decay creates 1000–1500 Frenkel-pair defects at room temperature, so that from the ^{243}Am half-life of $t_{1/2} = 7370$ years, we can estimate the number of the pair defects that accrue during the first 13 days to be 0.013–0.020 Frenkel pairs per unit cell. This number corresponds to only one pair defect per 50–75 unit cells on average.

At low temperatures, however, an even faster accumulation of the pair defects is anticipated, since the self-annealing effect by thermal diffusion processes is strongly suppressed. Indeed, x-ray-diffraction measurements on $^{243}AmO_2$ yielded a stronger lattice expansion, on the order of days, below 170 K [32]. Furthermore, unexpected broadening of the diffraction lines has been also observed below about 200 K. This broadening occurs reversibly and within a short period, on the order of an hour, suggesting that there is a much faster, but unknown, self-radiation damaging process in effect over a relatively wide range of samples. It has been inferred that such a process involves dislocations, such as rapid expansion of lattice strains around pair defects. The glassy nature of the magnetic transition might be related to such an unknown dislocating process. Further investigation of the self-radiation process (defects and strains), in particular in the low-temperature range, will be needed.

IV. SUMMARY

^{17}O NMR measurements have been performed on a newly synthesized $^{243}AmO_2$ powder sample. We have observed (i) the development of spatial inhomogeneity for static and dynamical susceptibilities in the paramagnetic state, (ii) signal wipeout in a wide temperature range below ~12 K, and (iii) a much broader NMR spectrum with a randomly distributed hyperfine field at the lowest temperature of 1.5 K. The results are all indicative of short-range, spin-glass-like character for the magnetic transition in this system. A fraction of the Am moments order in short-range and inhomogeneously created small clusters, while, in greater part, slow and distributed spin fluctuations persist down to very low temperatures. We have also observed a rapid change of the NMR line shape over the short-time interval of one month at 1.5 K. This can be understood by assuming a small shift of the distributed fluctuation spectrum to lower frequency to occur via sample aging.

Our NMR results clearly demonstrate that the electronic ground state of AmO_2 is extremely sensitive to disorder. On the other hand, we should not conclude that the spin-glass style of magnetic ordering observed here is "intrinsic" in this system. The present experiments were conducted over a time span of a few weeks after sample synthesis, and it seems that the radiation damage in that time interval is already enough to strongly impact the ground-state properties. It should also be remarked that, since Am^{4+} is a Kramers ion with an odd number of $5f$ electrons, AmO_2 should somehow be ordered magnetically in the ground state. The Curie-Weiss temperature $\theta = -70$ K from Knight-shift measurements indeed evidences that the system possesses substantial AFM exchange coupling between Am dipolar moments. Nonetheless, the slow Am moment fluctuations persisting down to very low temperatures is emblematic of the importance of magnetic frustration, possibly originating from the fcc structure of Am ions [46]. The fcc structure is known to be the simplest structure for a geometrically frustrated three-dimensional antiferromagnet [47–50]. Frustration often leaves the system fluctuating over a wide temperature region above the transition temperature. Such an effect might also be responsible for the broad $1/T_1$ maximum above T_0.

In this context, it is remarkable that the NMR behavior reported here for AmO_2 is very similar to that of a

geometrically frustrated antiferromagnet $NiGa_2S_4$. In the latter system the Ga NQR signal intensity gradually decreases with decreasing temperature and disappears (i.e., is wiped out) below ∼10 K, where the magnetic susceptibility shows a broad maximum [51]. With further decrease of temperature, extremely broad NQR spectra with a randomly distributed hyperfine field were observed below 2 K and almost half of Ga nuclei are undetectable due to the persistence of slow spin fluctuations, similar to our findings for AmO_2. $NiGa_2S_4$ is a two-dimensional triangular-lattice antiferromagnet, where geometrical frustration stabilizes the low-temperature spin-disordered state with slow dynamics [52]. Spin liquid formation has been proposed to be the origin of such exotic behavior [52,53]. The low-temperature magnetism of $NiGa_2S_4$ is also found to be extremely sensitive to both impurities and crystal imperfections [52,54,55]. We propose more comprehensive studies, with special monitoring of sample aging effects by specific heat, magnetic susceptibility, Mössbauer spectroscopy, and neutron scattering, in order to understand the unconventional electronic ground state of AmO_2.

ACKNOWLEDGMENTS

We thank M. Osaka, M. Kato, and M. T. Suzuki for valuable discussions and comments. A part of this work was supported by a Grant-in-Aid for Young Scientists (A) (Grant No. 23686137) by Japan Society for the Promotion of Science (JSPS), and a Grant-in-Aid for Scientific Research on Innovative Areas "Heavy Electrons" (Grants No. 20102006 and No. 20102007) by the Ministry of Education, Culture, Sports, Science and Technology of Japan, and the REIMEI Research Program of JAEA.

[1] B. T. Willis and R. I. Taylor, Phys. Lett. **17**, 188 (1965).
[2] B. C. Frazer, G. Shirane, D. E. Cox, and C. E. Olsen, Phys. Rev. **140**, A1448 (1965).
[3] P. Burlet, J. Rossat-Mignod, S. Quezel, O. Vogt, J. C. Spirlet, and J. Rebizant, J. Less-Common Met. **121**, 121 (1986).
[4] G. Amoretti, A. Blaise, R. Caciuffo, J. M. Fournier, M. T. Hutchings, R. Osborn, and A. D. Taylor, Phys. Rev. B **40**, 1856 (1989).
[5] K. Ikushima, S. Tsutsui, Y. Haga, H. Yasuoka, R. E. Walstedt, N. M. Masaki, A. Nakamura, S. Nasu, and Y. Ōnuki, Phys. Rev. B **63**, 104404 (2001).
[6] S. B. Wilkins, R. Caciuffo, C. Detlefs, J. Rebizant, E. Colineau, F. Wastin, and G. H. Lander, Phys. Rev. B **73**, 060406 (2006).
[7] S. Carretta, P. Santini, R. Caciuffo, and G. Amoretti, Phys. Rev. Lett. **105**, 167201 (2010).
[8] R. Caciuffo, P. Santini, S. Carretta, G. Amoretti, A. Hiess, N. Magnani, L.-P. Regnault, and G. H. Lander, Phys. Rev. B **84**, 104409 (2011).
[9] D. W. Osborne and E. F. Westrum, Jr., J. Chem. Phys. **21**, 1884 (1953).
[10] J. W. Ross and D. J. Lam, J. Appl. Phys. **38**, 1451 (1967).
[11] P. Santini and G. Amoretti, Phys. Rev. Lett. **85**, 2188 (2000).
[12] J. A. Paixão, C. Detlefs, M. J. Longfield, R. Caciuffo, P. Santini, N. Bernhoeft, J. Rebizant, and G. H. Lander, Phys. Rev. Lett. **89**, 187202 (2002).
[13] K. Kubo and T. Hotta, Phys. Rev. B **71**, 140404(R) (2005).
[14] K. Kubo and T. Hotta, Phys. Rev. B **72**, 132411 (2005).
[15] Y. Tokunaga, Y. Homma, S. Kambe, D. Aoki, H. Sakai, E. Yamamoto, A. Nakamura, Y. Shiokawa, R. E. Walstedt, and H. Yasuoka, Phys. Rev. Lett. **94**, 137209 (2005).
[16] Y. Tokunaga, D. Aoki, Y. Homma, S. Kambe, H. Sakai, S. Ikeda, T. Fujimoto, R. E. Walstedt, H. Yasuoka, E. Yamamoto, A. Nakamura, and Y. Shiokawa, Phys. Rev. Lett. **97**, 257601 (2006).
[17] R. Caciuffo, G. H. Lander, J. C. Spirlet, J. M. Fournier, and W. F. Kuhs, Solid State Commun. **64**, 149 (1987).
[18] J. M. Friedt, F. J. Litterst, and J. Rebizant, Phys. Rev. B **32**, 257 (1985).
[19] D. Mannix, G. H. Lander, J. Rebizant, R. Caciuffo, N. Bernhoeft, E. Lidström, and C. Vettier, Phys. Rev. B **60**, 15187 (1999).
[20] D. G. Karraker, J. Chem. Phys. **63**, 3174 (1975).
[21] G. M. Kalvius, S. L. Ruby, B. D. Dunlap, G. K. Shenoy, D. Cohen, and M. B. Brodsky, Phys. Lett. B **29**, 489 (1969).
[22] A. Bœuf, J. M. Fournier, J. F. Gueugnon, L. Manes, J. Rebizant, and F. Rustichelli, J. Phys. **40**, L335 (1979).
[23] M. M. Abraham, L. A. Boatner, C. B. Finch, and R. W. Reynolds, Phys. Rev. B **3**, 2864 (1971).
[24] W. Kolbe, N. Edelstein, C. B. Finch, and M. M. Abraham, J. Chem. Phys. **60**, 607 (1974).
[25] N. Magnani, P. Santini, G. Amoretti, and R. Caciuffo, Phys. Rev. B **71**, 054405 (2005).
[26] T. Hotta, Phys. Rev. B **80**, 024408 (2009).
[27] T. Hotta and H. Harima, J. Phys. Soc. Jpn. **75**, 124711 (2006).
[28] M.-T. Suzuki, N. Magnani, and P. M. Oppeneer, Phys. Rev. B **88**, 195146 (2013).
[29] K. Mendelssohn, E. King, J. A. Lee, M. H. Rand, C. S. Griffin, and R. S. Street, in *Plutonium*, edited by A. E. Kay and M. B. Waldron (Chapman and Hall, London, 1967), p. 189.
[30] T. D. Chikalla and R. P. Turcotte, Radiat. Eff. **19**, 93 (1973).
[31] W. J. Nellis, Inorg. Nucl. Chem. Lett. **13**, 393 (1977).
[32] U. Benedict and C. Dufour, Physica B **102**, 303 (1980).
[33] Y. Tokunaga, T. Nishi, S. Kambe, M. Nakada, A. Itoh, Y. Homma, H. Sakai, and H. Chudo, J. Phys. Soc. Jpn. **79**, 053705 (2010).
[34] I. D. Prodan, G. E. Scuseria, and R. L. Martin, Phys. Rev. B **76**, 033101 (2007).
[35] R. E. Walstedt, S. Kambe, Y. Tokunaga, and H. Sakai, J. Phys. Soc. Jpn. **76**, 072001 (2007).
[36] J. H. Cho, F. Borsa, D. C. Johnston, and D. R. Torgeson, Phys. Rev. B **46**, 3179 (1992).
[37] M. H. Julien, F. Borsa, P. Carretta, M. Horvatic, C. Berthier, and C. T. Lin, Phys. Rev. Lett. **83**, 604 (1999).
[38] A. Abragam, *The Principles of Nuclear Magnetism* (Oxford University Press, Oxford, 1961).
[39] A. Levitt and R. E. Walstedt, Phys. Rev. Lett. **38**, 178 (1977).
[40] D. E. MacLaughlin and H. Alloul, Phys. Rev. Lett. **38**, 181 (1977).
[41] M. C. Chen and C. P. Slichter, Phys. Rev. B **27**, 278 (1983).

[42] N. J. Curro, P. C. Hammel, B. J. Suh, M. Hucker, B. Buchner, U. Ammerahl, and A. Revcolevschi, Phys. Rev. Lett. **85**, 642 (2000).
[43] M.-H. Julien, A. Campana, A. Rigamonti, P. Carretta, F. Borsa, P. Kuhns, A. P. Reyes, W. G. Moulton, M. Horvatić, C. Berthier, A. Vietkin, and A. Revcolevschi, Phys. Rev. B **63**, 144508 (2001).
[44] G. B. Teitelbaum, I. M. Abu-Shiekah, O. Bakharev, H. B. Brom, and J. Zaanen, Phys. Rev. B **63**, 020507(R) (2000).
[45] A. W. Hunt, P. M. Singer, A. F. Cederström, and T. Imai, Phys. Rev. B **64**, 134525 (2001).
[46] The importance of the frustrated fcc structure has also been discussed in studies of the multipole ordered state in NpO_2; K. Kubo and T. Hotta, Phys. Rev. B **72**, 144401 (2005).
[47] See a review, for example, J. A. Mydosh, J. Magn. Magn. Mater. **7**, 237 (1978).
[48] G. S. Grest and E. G. Gabl, Phys. Rev. Lett. **43**, 1182 (1979).
[49] M. Matsuura, H. Hiraka, Y. Endoh, K. Hirota, and K. Yamada, Appl. Phys. A **74**, S792 (2002).
[50] M. Matsuura, Y. Endoh, H. Hiraka, K. Yamada, A. S. Mishchenko, N. Nagaosa, and I. V. Solovyev, Phys. Rev. B **68**, 094409 (2003).
[51] H. Takeya, K. Ishida, K. Kitagawa, Y. Ihara, K. Onuma, Y. Maeno, Y. Nambu, S. Nakatsuji, D. E. MacLaughlin, A. Koda, and R. Kadono, Phys. Rev. B **77**, 054429 (2008).
[52] S. Nakatsuji, Y. Nambu, H. Tonomura, O. Sakai, S. Jonas, C. Broholm, H. Tsunetsugu, Y. Qiu, and Y. Maeno, Science **309**, 1697 (2005).
[53] S. Nakatsuji, Y. Nambu, and S. Onoda, J. Phys. Soc. Jpn. **79**, 011003 (2010).
[54] Y. Nambu, S. Nakatsuji, and Y. Maeno, J. Phys. Soc. Jpn. **75**, 043711 (2006).
[55] Y. Nambu, S. Nakatsuji, Y. Maeno, E. K. Okudzeto, and J. Y. Chan, Phys. Rev. Lett. **101**, 207204 (2008).